Delft University of Technology

Study of TES Detector Transition Curve to Optimize the Pixel Design for Frequency-Division Multiplexing Readout

Ridder, M. L.; Nagayoshi, K.; Bruijn, M. P.; Gottardi, L.; Taralli, E.; Khosropanah, P.; Akamatsu, H.; van der Kuur, J.; Ravensberg, K.; Visser, S.

DOI
10.1007/s10909-020-02401-w

Publication date
2020

Document Version
Accepted author manuscript

Published in
Journal of Low Temperature Physics

Citation (APA)
Ridder, M. L., Nagayoshi, K., Bruijn, M. P., Gottardi, L., Taralli, E., Khosropanah, P., Akamatsu, H., van der Kuur, J., Ravensberg, K., Visser, S., Nieuwenhuizen, A. C. T., Gao, J. R., & den Herder, J. W. (2020). Study of TES Detector Transition Curve to Optimize the Pixel Design for Frequency-Division Multiplexing Readout. *Journal of Low Temperature Physics*, *199*(3-4), 962-967. https://doi.org/10.1007/s10909-020-02401-w

Important note
To cite this publication, please use the final published version (if applicable).
Please check the document version above.

Copyright
Other than for strictly personal use, it is not permitted to download, forward or distribute the text or part of it, without the consent of the author(s) and/or copyright holder(s), unless the work is under an open content license such as Creative Commons.

Takedown policy
Please contact us and provide details if you believe this document breaches copyrights.
We will remove access to the work immediately and investigate your claim.

This work is downloaded from Delft University of Technology.
For technical reasons the number of authors shown on this cover page is limited to a maximum of 10.

Journal of Low Temperature Physics
https://doi.org/10.1007/s10909-020-02401-w

Study of TES detector transition curve to optimize the pixel design for Frequency Division Multiplexing read-out

M.L. Ridder[1], K. Nagayoshi[1], M.P. Bruijn[1], L. Gottardi[1], E. Taralli[1], P. Khosropanah[1], H. Akamatsu[1], J. van der Kuur[1], K. Ravensberg[1], S. Visser[1], A.C.T. Nieuwenhuizen[1], J.R. Gao[1,2], J.-W. den Herder[1]

[1]*SRON Netherlands Institute for Space Research, The Netherlands*
[2]*Kavli Institute of NanoScience, Delft University of Technology, The Netherlands*

Abstract Superconducting transition-edge sensors (TESs) are highly sensitive detectors. Based on the outstanding performance on spectral resolution, the X-ray Integral Field Unit (X-IFU) instrument on-board Athena will be equipped with a large array of TES based microcalorimeters. For optimal performance in terms of the energy resolution, it is essential to limit undesirable non-linearity effects in the TES detector. Weak link behavior induced on the TES by superconducting leads is such a non-linearity effect. We designed and fabricated smart test structures to study the effect of the superconducting leads on the intrinsic transition curve of our TiAu based TES bilayer. We measured and analyzed the resistance versus temperature transition curves of the test structures. We found relations of long distance proximity effects with TES length and different lead materials. Based on these results, we can redesign and further optimize our TES based X-ray detectors.

Keywords Transition-edge sensors · Weak-link · Frequency-domain multiplexing

1 Introduction

SRON is developing a Frequency Domain Multiplexing (FDM) readout scheme for the X-IFU instrument [1]. In FDM readout experiments, non-linear behavior of a TES narrows the bias range in which optimal performance can be achieved, has been observed [2,3]. It has been concluded that the TESs act as superconducting weak-links due to the long distance lateral proximity effect originating from the superconducting leads, which are in direct contact with the TES bilayer. This long distance proximity effect was first reported by Sadleir et al. [4,5]. They found experimentally that when a TES is contacted to superconducting leads with a transition temperature (T_{cL}) above the intrinsic transition temperature of the bilayer (T_{ci}), superconductivity is induced longitudinally into the bilayer. This Longitudinal Proximity Effect was observed over extraordinarily long distances, exceeding 100 µm. Fig. 1 shows a schematic of a TES with two superconducting leads. We recapitulate some experimental findings of the work on MoAu TESs:

- The effective transition temperature (T_{ceff}) of the TES scales approximately as $1/L^2$, where L is the separation of the two leads, or equivalently, the length of the TES.
- The width of the temperature transition curve scales as $1/L^2$.
- The proximity effect is strongest near the leads and decays with distance away from the leads, with a minimum at $L/2$.
- The smaller the temperature difference between T_{cL} and T_{ci}, the smaller the impact of the lateral proximity effect.

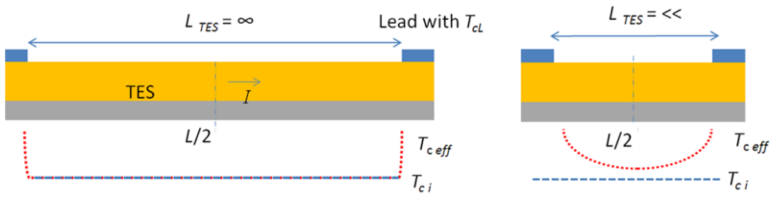

Fig. 1 On the left a schematic of a long TES with $L_{TES} >> L_{PROXIMITY}$ so that only a small fraction of the TES is influenced by the lateral proximity effect from the leads. On the right a schematic of a TES in the limit of short lead-to-lead separation, i.e. $L_{TES} << L_{PROXIMITY}$.The proximity effect induced by the leads can elevate the effective transition temperature T_{ceff} above T_{ci} over the whole length of the TES.

By investigating the effects of long distance proximity effects and thereby determining the length scales of the weak link behavior in our TiAu TES, we aim to further optimize our pixel design for Frequency Division Multiplexing read-out. In this paper we describe the impact of our standardly used Nb leads on the transition properties of the TiAu bilayer. Additionally, we will also investigate the effect by introducing lower T_{cL} leads of Ti instead of Nb.

2 Design of the test structures and experimental setup

To determine the length scale of the effect caused by the leads on the intrinsic transition curve of our TiAu bilayer, which has 35 nm Ti and 200 nm Au, we designed test structures with different TES lengths. In Fig. 2a an overview is shown of the test structures we used. To measure accurately T_{ci} and sheet resistance (R_{sqr}) of the bilayer, we included an extremely long TES with a length of 5000 µm, being much longer than $L_{PROXIMITY}$. Also other TES lengths closer to the regime of our standard TES detector dimensions, i.e. with lengths of 100, 50, 25 and 12.5 µm, respectively, were examined. The width of the TESs was kept constant at 50 µm. In order to distinguish the effect of the lead material, we produced two sets of test structures. One set with high T_c Nb leads (T_{cL} ~ 9 K), and one set with Ti leads (T_{cL} ~ 300 mK). Both the lead materials were patterned in lift-off mode and deposited by sputter deposition with in situ RF cleaning of the TES Au contact area. We used a standard AVS Resistance Bridge to measure resistance versus temperature R(T) curves. Above 10 µA excitation we observed self-heating effects judging from the observation of hysteresis and implausibly steep R (T) transition curves. Measurements at and below 3 µA excitation showed R (T) curves with shapes independent of the excitation level, and without hysteresis, and with many points in the transition curves. Based on this pre-test, we chose a fixed excitation current setting of 3 µA to measure all the samples. To increase the signal to noise ratio of the resistance measurement, the test structures consisted of 50 identical TESs in series. We first validated our test structures by comparing the shape and transition temperature of the R(T) curve of a single TES to the R(T) curve of 50 identical TESs in series. We found no changes in the shape nor the T_{ceff} of the transition curve (see Fig. 2b). This implies that we consider the results obtained in the 50 series array representative for the single TES case.

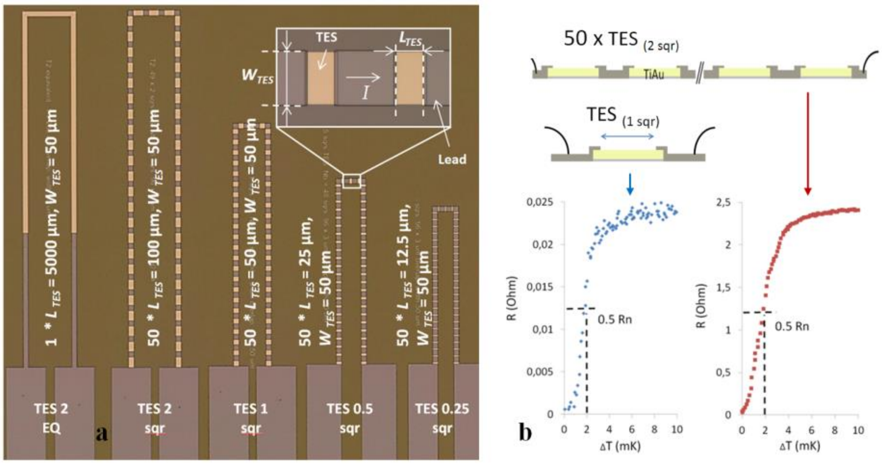

Fig. 2 The photo displays the 50 µm wide test structures with TES lengths of 5000, 100, 50, 25 and 12.5 µm, respectively. The leads connect to the TES bilayers on both sides with an overlap of 3 µm (a). Fig. 2 b: The transition curves show the comparison between a single square TES and series array of 50 x two square TESs, to validate the equivalence of the transition shape of both test structures.

3 Measured R(T) curves and analysis

For the TESs with L=5000 µm and with either Nb or Ti leads, we measured intrinsic transition temperatures T_{ci} of 110 and 100 mK, respectively. Both curves showed a steep (< 1 mK wide) transition. The small difference in T_{ci} is in consistence with the typical T_c spread obtained between different production batches. The normal state square resistance R_{sqr} of the TiAu bilayers was found to be R_{sqr} = 26 mΩ. The measured R(T) curves for all the test structures are shown in Fig. 3.

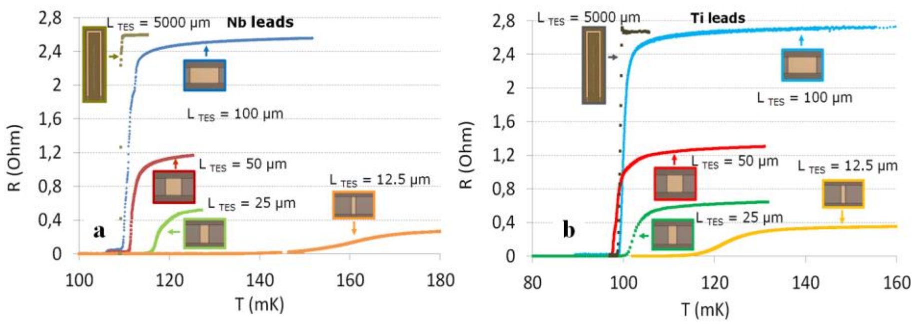

Fig. 3 R(T) curves of the TiAu bilayers with different TES lengths (L_{TES}) contacted with Nb leads (left), and with Ti leads (right), respectively.

For the TESs with Nb leads we observed a T_{ceff} close to T_{ci} (110 mK) for TESs with lengths of 50 and 100 µm. A clear increase in T_{ceff} was measured for the TESs with length of 25 µm (T_{ceff} = 116 mK), and for the TESs with length of 12.5 µm (T_{ceff} = 146 mK). For the TESs contacted with Ti leads, only the shortest TES length of 12.5 µm showed a clear increase in T_c from 100 mK (T_{ci}) to 116 mK (T_{ceff}).
To compare the transition curves of the TESs with Nb leads with the TESs with Ti leads, we have normalized the temperature and resistance data for both the subsets (see Fig. 4 a-d).

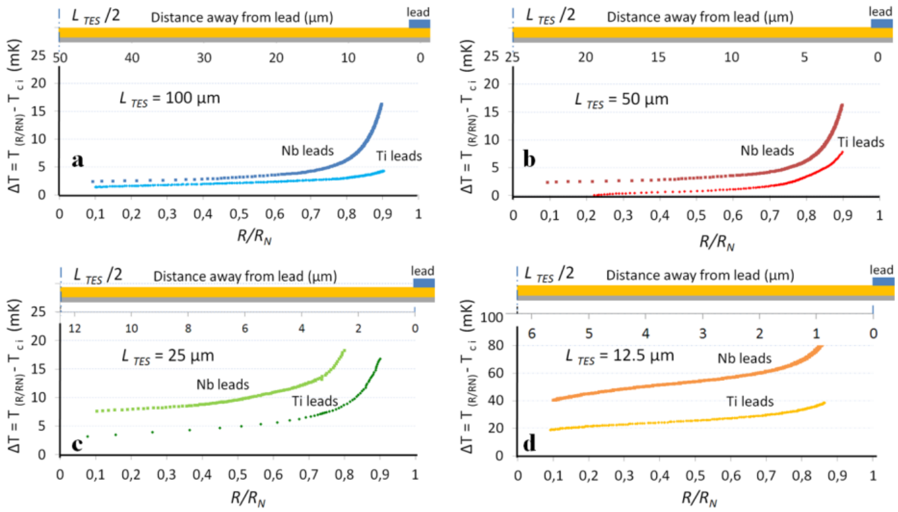

Fig. 4 Delta *T*, expressed as $T_{(R/RN)} - T_{ci}$, is plotted versus R/R_N and versus the distance from the lead (secondary horizontal axes above the graph) for different TES lengths of 100 µm (a), 50 µm (b), 25 µm (c) and 12.5 µm (d).

On the primary horizontal axis of the graphs in Fig. 4 we plotted the R/R_N value. Since we measured the R_{sqr} accurately, we could easily calculate the 100% normal state resistance value R_N for each test structure. On the vertical axis we plotted $\Delta T_R = T_{(R/RN)} - T_{ci}$, which is the difference between the temperature in the transition curve at a certain R/R_N ratio and the intrinsic transition temperature T_{ci}. The R/R_N value can also be considered as a measure for the fraction of the TES region that becomes normal at a certain temperature. By assuming the proximity effect is increased near the leads and decays with distance away from the leads to a minimum at *L/2*, the R/R_N values can be converted to distance units of TES length. In this way we can

add a secondary horizontal axis showing the distance in µm from the lead contact towards the center at *L/2* of the TES bilayer. As can be seen, ΔT_R is at highest within 10 µm from the leads, especially for the Nb leads. More than 30 micron away from the leads the proximity effect is diminished for both the lead materials.
To verify for typical length scaling of the lateral proximity effect we plotted the transition width expressed as $\Delta T = T_{(R/RN = 0.8)} - T_{(R/RN = 0.1)}$ versus the length of the TES (Fig. 5a). The width of the transition scales roughly with $1/L^2$. Less broadening of the transition was observed by the TESs connected with Ti leads; for the short TESs (L = 12.5 µm) with Ti leads the transition width is 12 mK versus 29 mK for the TESs with Nb leads.

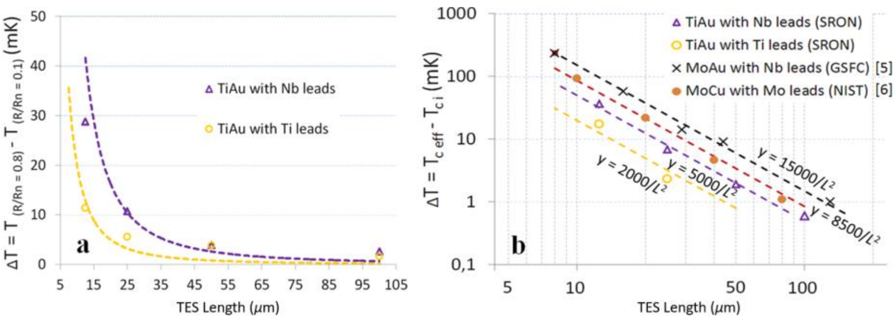

Fig. 5 The graph on the left (a) shows the width of the transition curve defined as $\Delta T = T_{(R/RN = 0.8)} - T_{(R/RN = 0.1)}$ versus TES length. On the right side (b) the $\Delta T = T_{ceff} - T_{ci}$ is plotted as a function of the TES lengths.

In Figure 5b the difference between the T_{ceff} and the T_{ci} is displayed for various TES lengths and various lead materials. In the graph we also included a selection of data points (measured with the same current density) reported by other groups [5,6]. The fitted $1/L^2$ curves in the graph show that there is agreement with the weak link model for the TESs with lengths ranging from 12.5 to 50 µm. For TESs with lengths exceeding 50 µm the elevation of the effective T_c of the TES as a result of the weak link effect, vanishes and becomes indistinguishable from the intrinsic spread of T_{ci}.
From a comparison of the effects of different lead materials for TESs of the same size, we can conclude that the characteristic length scale of the proximity effect is the lowest for the TiAu TES with Ti leads, i.e. T_{ceff} minus T_{ci} is about 2.5 higher for the TiAu TES with Nb leads, and almost 8 times higher for the MoAu TES with Nb leads. Since the size of the TESs is the same, the difference between the data sets must originate from difference in lead material, TES to lead interface conditions, but also by material properties as intrinsic coherence length of the bilayer.

https://doi.org/10.1007/s10909-020-02401-w

4 Conclusions

We experimentally studied longitudinal proximity effects in our TiAu bilayers induced by the superconducting leads. We found how the long distance proximity effect relates to the TES length. We also found that Nb leads have a stronger proximity effect on the TES than Ti leads. The results are in agreement with the explanation of the lateral proximity model. Based on these results we can redesign and further optimize our TES based X-ray detectors.

Acknowledgements

This work is partly funded by European Space Agency (ESA) under ESA CTP contract ITT AO/1-7947/14/NL/BW, and is partly funded by the European Union's Horizon 2020 Program under the AHEAD project with grant agreement number 654215.

References

1. D. Barret et al., In Proc. SPIE Space Telescopes and Instrumentation 2016: Ultraviolet to Gamma Ray (2016)
2. L. Gottardi , H. Akamatsu, M. Bruijn, J. R. Gao, R. den Hartog, R. Hijmering, H. Hoevers, P. Khosropanah, A. Kozorezov, J. van der Kuur, A. van der Linden, M. Ridder J Low Temp Phys (2014) **176**:279–284
3. L. Gottardi, et al., *IEEE Trans. Appl. Superc*. (2017).
4. J. E. Sadleir, S. J. Smith, S. R. Bandler, J. A. Chervenak, and J. R. Clem, *Phys. Rev. Lett.* **104**, 047003 (2010)
5. J. E. Sadleir, S. J. Smith, K. Robinson, F. M. Finkbeiner, J. A. Chervenak, S. R. Bandler, M. E. Eckart, C. A. Kilbourne, *Phys. Rev*. B **84** 184502 (2011)
6. Ullom, Joel N., and Douglas A. Bennett. Supercond. Sci. Technol.**28** (2015) 084003